Electronic supplementary materials *Mendeleev Commun.*, 2026, **36**, 1–11

Design and biomedical applications of fluorescent probes based on hemicyanine dyes

Mariya A. Ustimova and Olga A. Fedorova

Compound	λ_{max}^{abs} [1] (nm)	λ_{max}^{fl} [2] (nm)	φ^{fl} [3]	Research, potential application area	Ref.
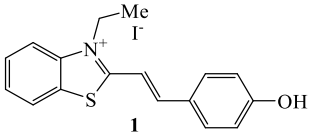 **1**	405	514	0.0002	- specific localization in lysosomes;	S1
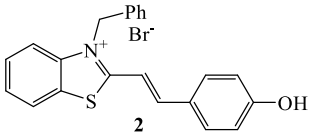 **2**	415	520	0.0004	- specific localization in lysosomes;	S1
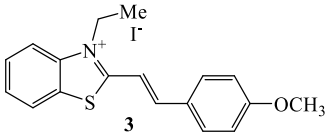 **3**	405	510	0.0001	- specific localization in lysosomes;	S1
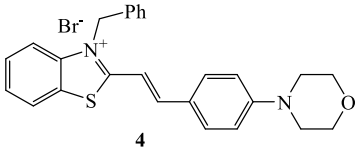 **4**	454	597	0.002	- simultaneously stains both cellular lysosomes and mitochondria;	S2
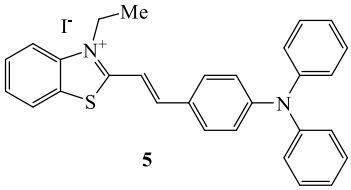 **5**	501	720	0.0001	- significant enhancement of fluorescence upon interaction with albumin; - lysosomal selectivity;	S3, S4
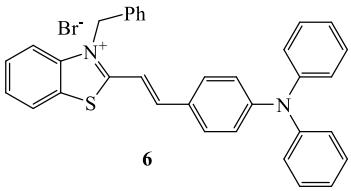 **6**	517	731	0.0001	- significant enhancement of fluorescence upon interaction with albumin; - lysosomal selectivity;	S3, S4
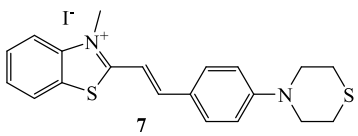 **7**	490	590	-*	- the quantum yield of fluorescence increased many times in the presence of double-stranded DNA; - the dye targets the nucleoli and endoplasmic reticulum of the cell;	S5

[1] - for most examples, maximum absorption band in aqueous solution or buffer are presented

[2] - for most examples, maximum of fluorescence band in aqueous solution or buffer are presented

[3] - for most examples, the quantum yield of fluorescence in aqueous solution or buffer are presented

* - data not presented in the article

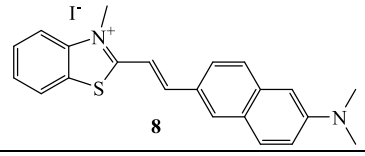 **8**	488	690	-*	- localized in the cell's mitochondria; - can be used to detect both exogenous and endogenous SO_2 derivatives in living cells;	S6
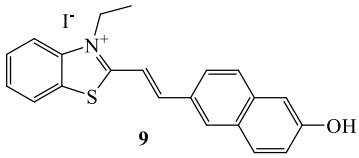 **9**	419	559	-*	- can be used to detect exogenous and endogenous HSO_3^- in living cells;	S7
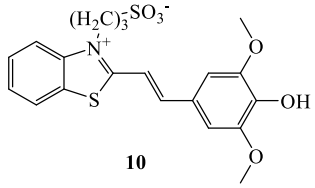 **10**	432/ 560	550/ 604	-*	- did not show selective localization in mitochondria;	S7
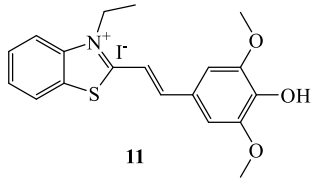 **11**	423/ 549	547/ 600	-*	- sensitive to pH changes; - can be successfully used to record changes in the mitochondrial microenvironment in cardiomyocytes (heart muscle cells) caused by the presence of Zn^{2+} cations;	S7, S8
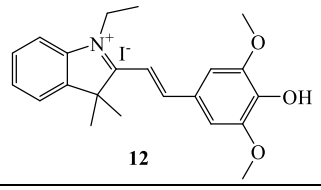 **12**	569	595	-*	- demonstrated the weakest response to HSO_3^- recognition;	S7
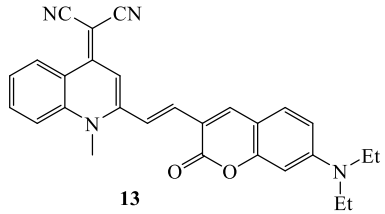 **13**	447	695	0.0004	- with an increase in the viscosity of the medium from 0.89 cP to 856 cP, the fluorescence intensity increases by 418 times; - a promising candidate for studies of dynamic pathological processes associated with mitophagy;	S9
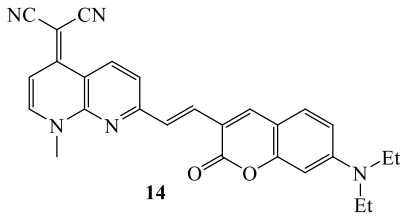 **14**	451	720	0.0007	- with an increase in the viscosity of the medium from 0.89 cP to 856 cP, the fluorescence intensity increases by 769 times; - a promising candidate for studies of dynamic pathological processes associated with mitophagy;	S9
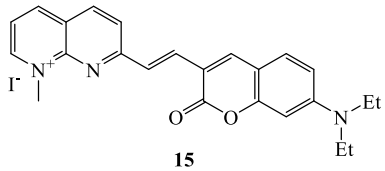 **15**	521	-[4]	-[4]	- increased fluorescence intensity upon interaction with DNA and RNA; - localization in mitochondria of fixed cells;	S10
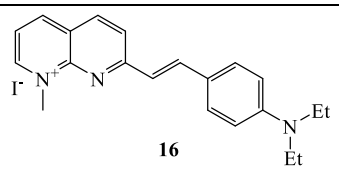 **16**	458	-[4]	-[4]	- increase in fluorescence intensity, namely 143 and 127 times when interacting with DNA and RNA, respectively; - localization in mitochondria of fixed cells;	S10

[4] - not detected

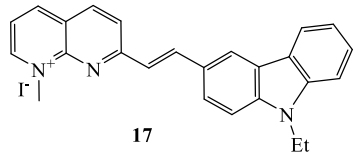 **17**	528	-[4]	-[4]	- increased fluorescence intensity upon interaction with DNA and RNA; - localization in mitochondria of fixed cells;	S10
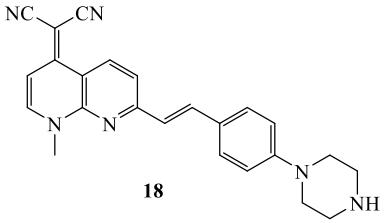 **18**	485	679	0.011	- sensitivity of fluorescence to medium viscosity; - localized in the lysosome region of the cell;	S11
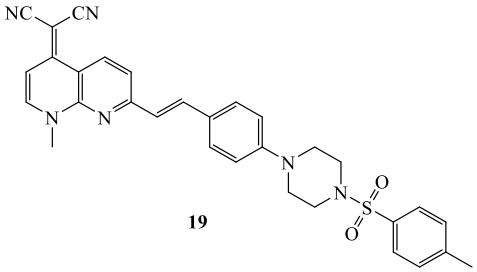 **19**	492	661	0.036	- sensitivity of fluorescence to medium viscosity; - localized in the region of the endoplasmic reticulum of the cell; - demonstrated the ability to migrate from the endoplasmic reticulum to lysosomes during hydrogen peroxide-induced cell damage;	S11
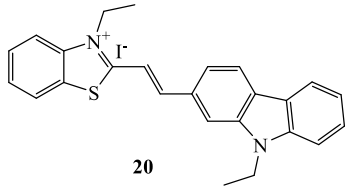 **20**	453	584	-*	- fluorescence intensity increased significantly in the presence of different types of nucleic acids (NA); - exhibits high selectivity for DNA; - mainly concentrated in the cell nucleus;	S12
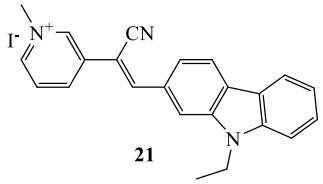 **21**	405	559	-*	- fluorescence intensity increased significantly in the presence of different types of nucleic acids (NA); - can simultaneously bind to both G-quadruplex DNA and RNA; - predominantly stains the cytoplasm;	S12
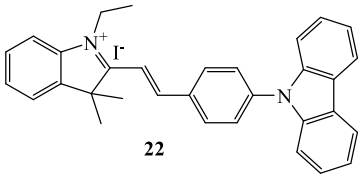 **22**	~475[5]	~575[5]	0.0003[5]	- localizes to mitochondria and can be used to monitor changes in viscosity;	S13
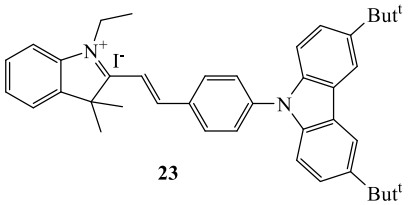 **23**	~515/ 550[5]	~575[5]	0.0022[5]	- localizes to mitochondria and can be used to monitor changes in viscosity;	S13
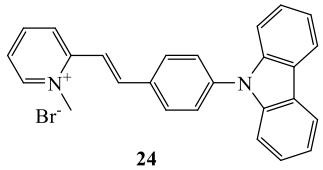 **24**	402	545	-*	- can distinguish G-quadruplex from duplex and single-stranded DNA;	S14
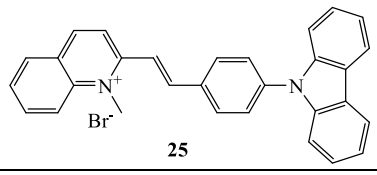 **25**	-*	-*	-*	- showed low selectivity for these DNA types;	S14

[5] - optical properties were studied in ethanol solution

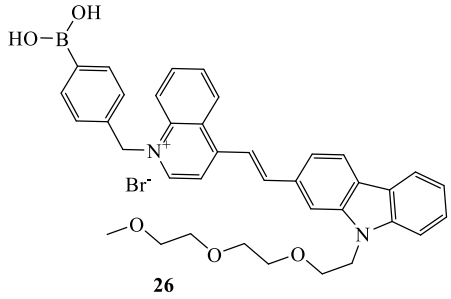 **26**	476	605	-*	- exhibits the ability to stabilize the G-quadruplex DNA structure to some extent, primarily through stacking with terminal heterocyclic DNA fragments; - localization of the dye in the cytoplasm of living cells;	S15
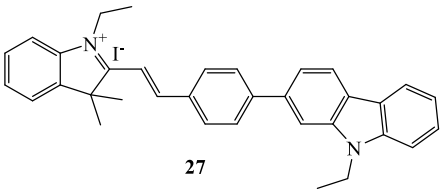 **27**	~500[6]	-*	0.0002[6]	- is able to visualize changes in mitochondrial viscosity during the development of the inflammatory process at the level of cells and organisms of zebrafish and mice;	S16
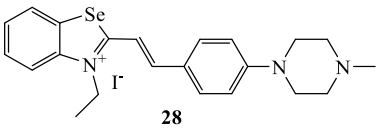 **28**	458	580	0.0063	- when bound to a biomolecule, it exhibited a moderate bathochromic and hypochromic shift in the absorption spectra, a significant increase in fluorescence intensity; - localization in lysosomes;	S17
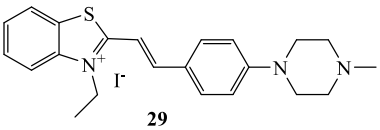 **29**	443	570	0.0152	- when bound to a biomolecule, it exhibited a moderate bathochromic and hypochromic shift in the absorption spectra, a significant increase in fluorescence intensity; - localization in mitochondria;	S17
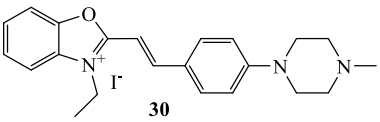 **30**	430	536	-[4]	- when bound to a biomolecule, it exhibited a moderate bathochromic and hypochromic shift in the absorption spectra, a significant increase in fluorescence intensity; - localization in mitochondria;	S17
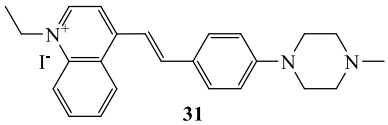 **31**	437	640	0.0081	- when bound to a biomolecule, it exhibited a moderate bathochromic and hypochromic shift in the absorption spectra, a significant increase in fluorescence intensity; - localization in mitochondria;	S17
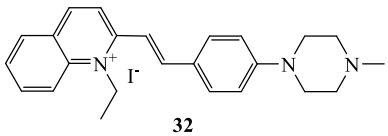 **32**	430	600	0.0018	- when bound to a biomolecule, it exhibited a moderate bathochromic and hypochromic shift in the absorption spectra, a significant increase in fluorescence intensity; - localization in mitochondria;	S17
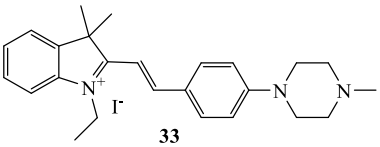 **33**	478	572	0.0032	- when bound to a biomolecule, it demonstrated a moderate bathochromic and hypochromic shift in the absorption spectra, a significant increase in fluorescence intensity; - localization in mitochondria;	S17

[6] - optical properties were studied in methanol solution

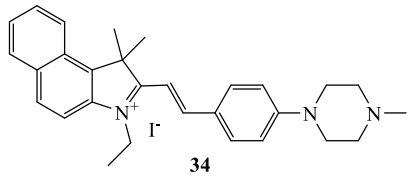 **34**	490	590	0.0029	- when bound to a biomolecule, it demonstrated a moderate bathochromic and hypochromic shift in the absorption spectra, a significant increase in fluorescence intensity; - equal distribution between mitochondria and lysosomes; - exhibited moderate cytotoxicity even at micromolar concentrations;	S17
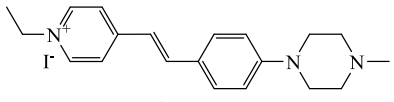 **35**	395	577	0.0238	- when bound to a biomolecule, it demonstrated a moderate bathochromic and hypochromic shift in the absorption spectra, a significant increase in fluorescence intensity; - localization in mitochondria;	S17
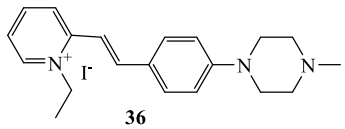 **36**	383	556	0.0059	- when bound to a biomolecule, it demonstrated a moderate bathochromic and hypochromic shift in the absorption spectra, a significant increase in fluorescence intensity; - localization in mitochondria;	S17
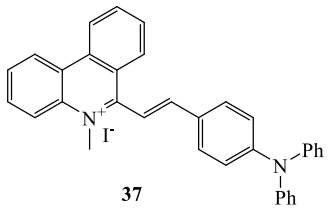 **37**	467	647	0.0093	- with an increase in viscosity from 0.89 cP to 856 cP, the fluorescence intensity in glycerol increased by 115 times; - high photostability, low cytotoxicity and localization in the mitochondria; - can detect changes in mitochondrial viscosity during autophagy induced by rapamycin and nystatin;	S18
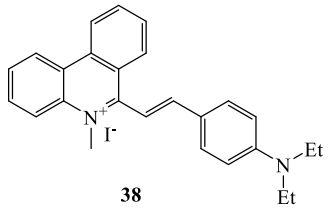 **38**	501	646	0.0052	- with an increase in viscosity from 0.89 cP to 856 cP, the fluorescence intensity in glycerol increased by 83 times; - high photostability, low cytotoxicity and localization in the mitochondria;	S18
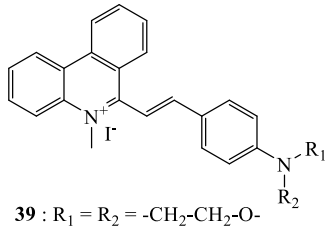 **39** : $R_1 = R_2 =$ -CH_2-CH_2-O-	411	641	0.0042	- with an increase in viscosity from 0.89 cP to 856 cP, the fluorescence intensity in glycerol increased by 303 times; - high photostability, low cytotoxicity and localization in the mitochondria;	S18
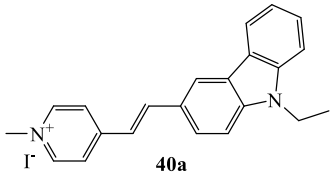 **40a**	419	595	0.0168	- fluorescence intensity increased in aprotic and viscous media; - minor cytotoxicity and localization in the cell mitochondria;	S19
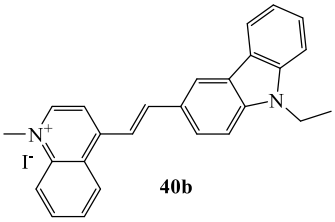 **40b**	459	658	0.0032	- fluorescence intensity increased in aprotic and viscous media; - minor cytotoxicity and localization in the cell mitochondria;	S19

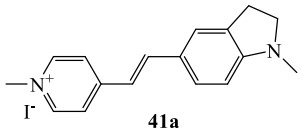 **41a**	430	637	0.0016	- fluorescence intensity increased in aprotic and viscous media; - minor cytotoxicity and localization in the cell mitochondria; - can be used to identify pathological cell conditions by demonstrating changes in fluorescence during mitophagy;	S19, S20
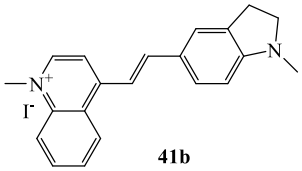 **41b**	484	726	0.0003	- fluorescence intensity increased in aprotic and viscous media; - minor cytotoxicity and localization in the cell mitochondria;	S19
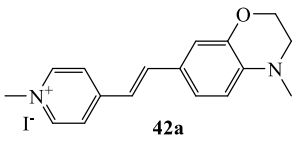 **42a**	446	638	0.0016	- fluorescence intensity increased in aprotic and viscous media; - minor cytotoxicity and localization in the cell mitochondria;	S19
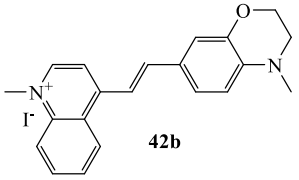 **42b**	505	718	0.0005	- fluorescence intensity increased in aprotic and viscous media; - minor cytotoxicity and localization in the cell mitochondria;	S19
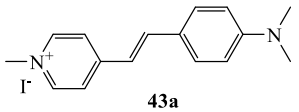 **43a**	449	616	0.0022	- fluorescence intensity increased in aprotic and viscous media; - minor cytotoxicity and localization in the cell mitochondria;	S19
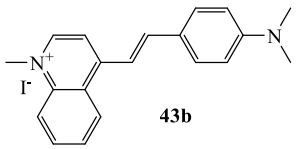 **43b**	510	694	0.0005	- fluorescence intensity increased in aprotic and viscous media; - minor cytotoxicity and localization in the cell mitochondria;	S19
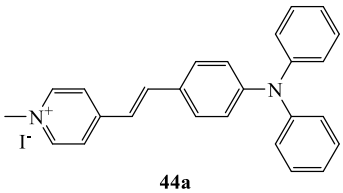 **44a**	451	650	0.0006	- fluorescence intensity increased in aprotic and viscous media; - minor cytotoxicity and localization in the cell mitochondria;	S19
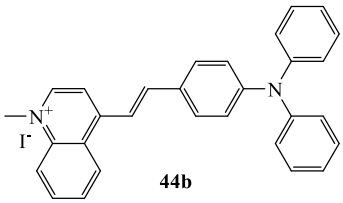 **44b**	494	728	0.0004	- fluorescence intensity increased in aprotic and viscous media; - minor cytotoxicity and localization in the cell mitochondria;	S19
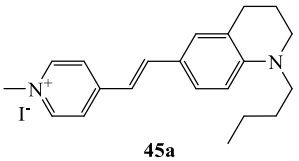 **45a**	485	632	0.0023	- fluorescence intensity increased in aprotic and viscous media; - minor cytotoxicity and localization in the cell mitochondria; - can be used to identify pathological cell conditions by demonstrating changes in fluorescence during mitophagy;	S19, S20
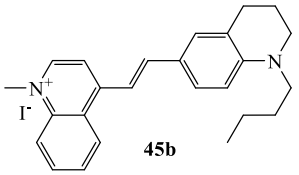 **45b**	554	713	0.0007	- fluorescence intensity increased in aprotic and viscous media; - minor cytotoxicity and localization in the cell mitochondria;	S19

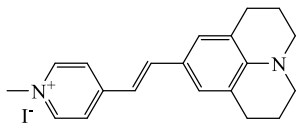 **46a**	491	644	0.0014	- fluorescence intensity increased in aprotic and viscous media; - minor cytotoxicity and localization in the cell mitochondria;	S19
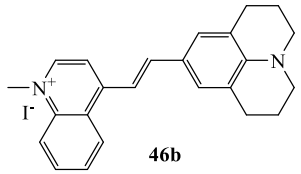 **46b**	568	730	0.0005	- fluorescence intensity increased in aprotic and viscous media; - minor cytotoxicity and localization in the cell mitochondria;	S19
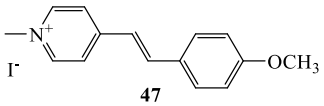 **47**	373	501	0.0120	- interacts with ds-DNA by intercalation;	S21
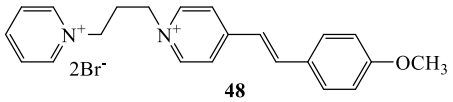 **48**	382	511	0.0336	- interacts with ds-DNA by inserting into the minor groove;	S21
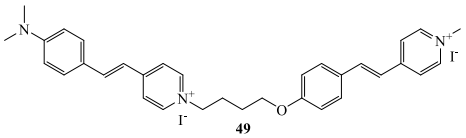 **49**	380/ 471	502/ 610	0.0012	- demonstrate a 151-fold increase in fluorescence in DNA solutions, while in the presence of RNA the increase effect is significantly lower (23 times);	S22
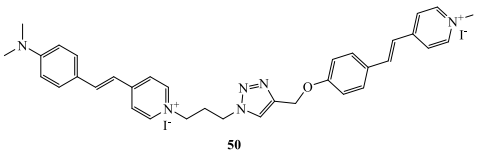 **50**	380/ 482	508/ 617	0.0008	- demonstrate a 118-fold increase in fluorescence in DNA solutions, while in the presence of RNA the increase effect is significantly lower (36 times);	S22
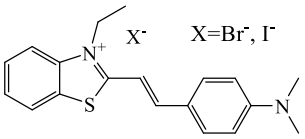 **51**	513	598	0.0025	- demonstrated localization in the mitochondria of living cells;	S23
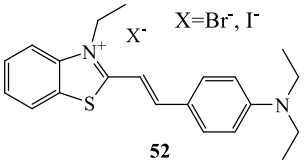 **52**	523	601	0.0024	- demonstrated localization in the mitochondria of living cells;	S23
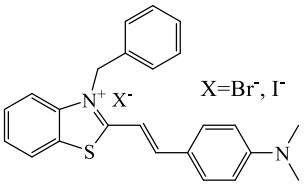 **53**	528	603	0.0017	- demonstrated localization in the mitochondria of living cells;	S23
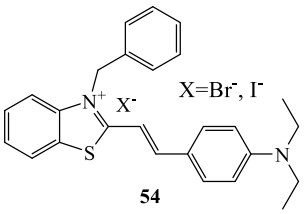 **54**	538	609	0.0024	- demonstrated localization in the mitochondria of living cells;	S23
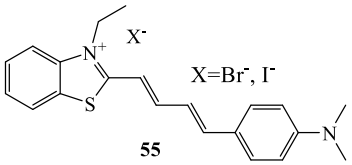 **55**	521	699	0.0046	- demonstrated localization in the mitochondria of living cells; - high biocompatibility and rapid staining;	S23

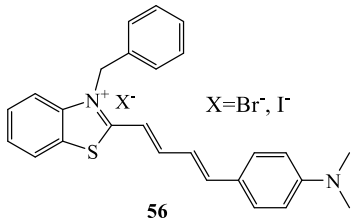 **56**	541	706	0.0035	- demonstrated localization in the mitochondria of living cells;	S23
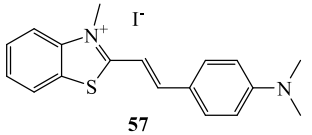 **57**	510	593	-[4]	- increase in fluorescence intensity with increasing solvent viscosity; - bioconjugate with dye can visualize β-amyloid in the brain of transgenic mouse with Alzheimer's disease;	S24
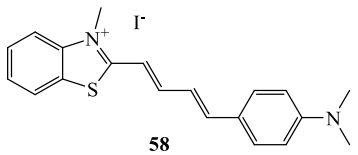 **58**	521	688	-[4]	- increase in fluorescence intensity with increasing solvent viscosity; - bioconjugate with dye can visualize β-amyloid in the brain of transgenic mouse with Alzheimer's disease;	S24
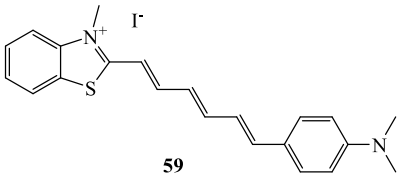 **59**	518	803	-[4]	- increase in fluorescence intensity with increase in solvent viscosity; - fluorescence intensity is quite low;	S24
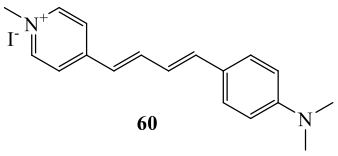 **60**	447	709	0.0056	- when complexed with polynucleotides, a noticeable increase in fluorescence was observed; - in in vitro experiments, the dyes demonstrated selective staining of RNA, localizing in the nucleoli and mitochondria of the cell;	S25
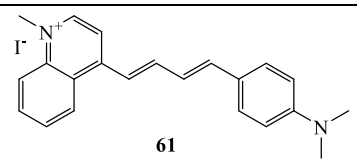 **61**	511	688	0.002	- when complexed with polynucleotides, a noticeable increase in fluorescence was observed; - in in vitro experiments, the dyes demonstrated selective staining of RNA, localizing in the nucleoli and mitochondria of the cell; - moderate antiproliferative effect on two tumor cell lines (A549 and HT-29);	S25
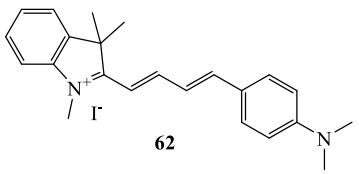 **62**	577	684	0.008	- selective detection of human serum albumin (HSA);	S26, S27
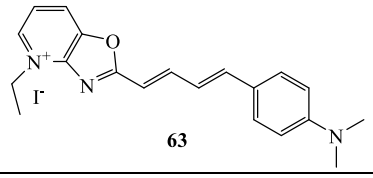 **63**	501	697	0.004	-	S27
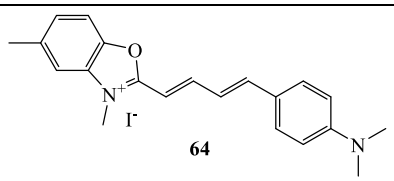 **64**	505	651	0.025	-	S27

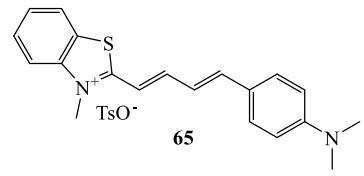 **65**	524	684	0.010	- has better photo- and thermal stability compared to other dyes of the series (62-67); - exhibits greater selectivity for RNA staining and can also be used as a near-infrared fluorescent probe for nuclear imaging of living cells;	S27
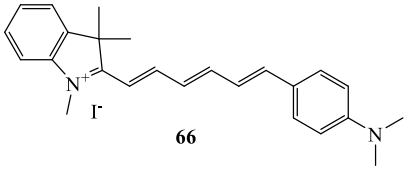 **66**	568	790	0.002	-	S27
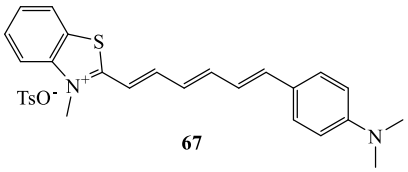 **67**	519	786	0.002	-	S27
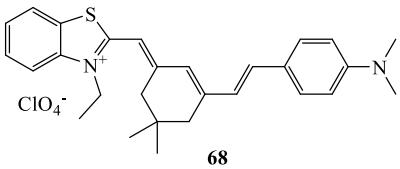 **68**	590	785	-*	- sensitive to local changes in the environment; - when complexing with a DNA biomolecule, a hypsochromic shift of the fluorescence maximum and a multiple increase in intensity were observed in the emission spectrum, which confirms the binding of the dye to the biomolecule. Also, the interaction of the dye with DNA was accompanied by an increase in the average fluorescence lifetime;	S28
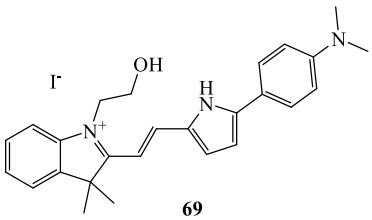 **69**	610[7]	725[7]	0.0058[7]	- showed the greatest intensity of increase in fluorescent response to viscosity and binding to β-amyloid (from series 69-72); - localizes in the mitochondria of the cell; - showed a 1.56-fold increase in fluorescent response to β-amyloid plaques in the mouse brain	S29
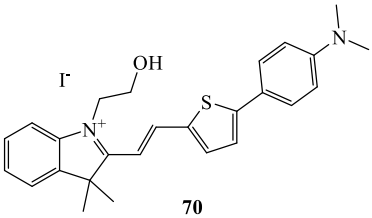 **70**	600[7]	770[7]	0.041[7]	-	S29
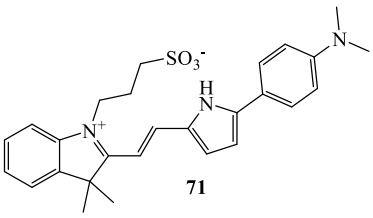 **71**	610[7]	725[7]	0.011[7]	-	S29

[7] - optical properties were studied in DMSO.

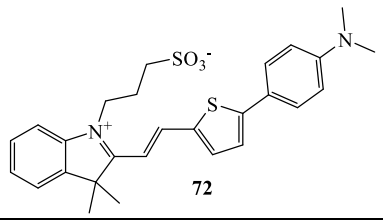 72	600[7]	770[7]	0.075[7]	-	S29
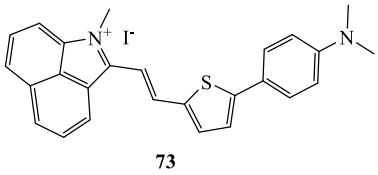 73	~630	980[8]	-*	- showed a specific increase in fluorescence (41.8 times) when binding to β-amyloid fibrils; - demonstrated a significant difference in fluorescence intensity in the brain of a mouse with Alzheimer's disease and compared to fluorescence in the brain of a control healthy mouse after injection of the dye;	S30
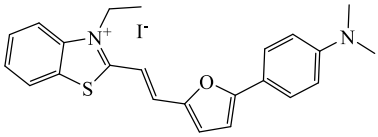 74	532	793	0.007	- was successfully used for visual identification of mitochondrial dysfunction due to membrane potential disturbance in living cells;	S31

References

S1 C. S. Abeywickrama, K. A. Bertman, L. J. Mcdonald, N. Alexander, D. Dahal, H. J. Baumann, C. R. Salmon, C. Wesdemiotis, M. Konopka, C. A. Tessier and Y. Pang, *J. Mater. Chem. B*, 2019, **7**, 7502.

S2 C. S. Abeywickrama, H. J. Baumann and Y. Pang, *J. Fluoresc.*, 2021, **31**, 1227.

S3 C. S. Abeywickrama, H. J. Baumann, K. A. Bertman, B. Corbin and Y. Pang, *Biosensors*, 2022, **12**, 504.

S4 C. S. Abeywickrama, Y. Li, A. Ramanah, D. N. Owitipana, K. J. Wijesinghe and Y. Pang, *Sensors Actuators B Chem.*, 2022, **368**, 132199.

S5 A. A. Vasilev, M. Miteva, N. Ishkitiev, M. Dragneva, L. Topalova and M. I. Kandinska, *Molbank*, 2022, **2022**, M1392.

S6 H. Huang, W. Liu, X. J. Liu, Y. Q. Kuang and J. H. Jiang, *Talanta*, 2017, **168**, 203.

S7 B. Y. Zhang, X. F. Zhang, X. Y. Ma, D. W. Yang, H. X. Sun, Y. L. Tang and L. Shi, *J. Org. Chem.*, 2023, **88**, 9959.

S8 B.-y. Zhang, P. Wang, L. Shi, X.-y. Ma, J.-k. Xi and X.-f. Zhang, *Microchem. J.*, 2023, **193**, 109085.

S9 J. Y. Zhao, G. Zhang, H. C. Hao, R. Sun, Y. J. Xu and J. F. Ge, *Sensors Actuators B Chem.*, 2024, **401**, 135010.

S10 H. Ma, W. P. Ni, Q. Lin, R. Sun and J. F. Ge, *Analyst*, 2025, **150**, 642.

S11 H. Wang, J. Y. Zhao, R. Sun and J. F. Ge, *Microchem. J.*, 2025, **212**, 113344.

S12 G. Hao, J. Sun and C. Wei, *Bioorg. Med. Chem.*, 2018, **26**, 285.

[8] - optical properties were studied in an organic solvent (DCM/MeOH)

S13 K. Zhou, M. Ren, B. Deng and W. Lin, *New J. Chem.*, 2017, **41**, 11507.

S14 M. Q. Wang, G. Y. Ren, S. Zhao, G. C. Lian, T. T. Chen, Y. Ci and H. Y. Li, *Spectrochim. Acta Part A Mol. Biomol. Spectrosc.*, 2018, **199**, 441.

S15 J. Li, Q. Yang, L. Zhao, M. Xu and H. Zhang, *Tetrahedron Lett.*, 2021, **70**, 153004.

S16 J. Yin, M. Peng and W. Lin, *Anal. Chem.*, 2019, **91**, 8415.

S17 I. Čipor, A. Kurutos, G. M. Dobrikov, F. S. Kamounah, D. Majhen, D. Nestić and I. Piantanida, *Dye. Pigment.*, 2022, **206**, 110626.

S18 H. X. Wang, J. Y. Zhao, H. Wang, H. Ma, J. F. Ge and R. Sun, *Dye. Pigment.*, 2025, **232**, 112479.

S19 A. S. Efimova, M. A. Ustimova, N. S. Chmelyuk, M. A. Abakumov, Y. V. Fedorov and O. A. Fedorova, *Biosensors*, 2023, **13**, 734.

S20 A. S. Efimova, M. A. Ustimova, A. Y. Frolova, V. I. Martynov, S. M. Deyev, Y. V. Fedorov, O. A. Fedorova and A. A. Pakhomov, *Opt. Mater. (Amst).*, 2025, **159**, 116517.

S21 M. A. Ustimova, P. A. Chernikova, N. E. Shepel, Y. V. Fedorov and O. A. Fedorova, *Mendeleev Commun.*, 2020, **30**, 217.

S22 M. A. Ustimova, Y. V. Fedorov, N. S. Chmelyuk, M. A. Abakumov and O. A. Fedorova, *Spectrochim. Acta Part A Mol. Biomol. Spectrosc.*, 2022, **279**, 121446.

S23 C. S. Abeywickrama, H. J. Baumann, N. Alexander, L. P. Shriver, M. Konopka and Y. Pang, *Org. Biomol. Chem.*, 2018, **16**, 3382.

S24 L. Ma, S. Yang, Y. Ma, Y. Chen, Z. Wang, T. D. James, X. Wang and Z. Wang, *Anal. Chem.*, 2021, **93**, 12617.

S25 A. Cesaretti, E. Calzoni, N. Montegiove, T. Bianconi, M. Alebardi, M. A. La Serra, G. Consiglio, C. G. Fortuna, F. Elisei and A. Spalletti, *Int. J. Mol. Sci.*, 2023, **24**, 4812.

S26 S. I. Reja, I. A. Khan, V. Bhalla and M. Kumar, *Chem. Commun.*, 2016, **52**, 1182.

S27 J. T. Miao, C. Fan, R. Sun, Y. J. Xu and J. F. Ge, *J. Mater. Chem. B*, 2014, **2**, 7065.

S28 S. Udayan, V. K. Ramachandran, M. Sebastian, P. Chandran, V. P. N. Nampoori and S. Thomas, *Opt. Mater. (Amst).*, 2017, **69**, 49.

S29 W. Wang, Z. Mo, L. Han, H. Zuo, Y. Chen, Y. Fang, X. Li, K. Wang and J. Pan, *Eur. J. Med. Chem.*, 2025, **281**, 117001.

S30 J. Miao, M. Miao, Y. Jiang, M. Zhao, Q. Li, Y. Zhang, Y. An, K. Pu and Q. Miao, *Angew. Chemie Int. Ed.*, 2023, **62**, e202216351.

S31 K. A. Bertman, C. S. Abeywickrama and Y. Pang, *ChemBioChem*, 2022, **23**, e202100516.